Title: The economic strategies of superorganisms

Lily Leahy[1*], Hannah L. Riskas[1], Ben Halliwell[2,3], Ian J. Wright[4,5], Amelia G. Carlesso[1,6], Nathan J. Sanders[7], Tom R. Bishop[8,9], Catherine L. Parr[9,10], Steven L. Chown[11], Alan N. Andersen[12], Heloise Gibb[6, 13]

1 Department of Ecological, Plant, and Animal Sciences, La Trobe University, Bundoora, VIC, Australia
2 Biological Sciences, School of Natural Sciences, University of Tasmania, Hobart, TAS, Australia
3 ARC Centre of Excellence for Plant Success in Nature and Agriculture, University of Tasmania, Hobart, TAS, Australia
4 Hawkesbury Institute for the Environment, Western Sydney University, Penrith, NSW, Australia
5 School of Natural Sciences, Macquarie University, North Ryde, NSW Australia
6 School of Life and Environmental Sciences, Deakin University, Burwood, VIC, Australia
7 Department of Ecology and Evolutionary Biology, University of Michigan, Ann Arbor, MI, USA
8 School of Biosciences, Cardiff University, Cardiff, UK
9 Department of Zoology and Entomology, University of Pretoria, Pretoria, South Africa
10 School of Environmental Sciences, University of Liverpool, Liverpool, UK
11 School of Biological Sciences, Monash University, Monash, Victoria 3800, Australia
12 Research Institute for the Environment and Livelihoods, Charles Darwin University, Palmerston, NT, Australia
13 School of Biological, Earth and Environmental Sciences (BEES), UNSW, Kensington NSW, Australia

Corresponding author

*Lily Leahy: lilyleahy4@gmail.com

Orcid: 0000-0002-0733-6792

Summary

Economic principles can be applied to biological life to understand how resource allocation strategies maximise evolutionary fitness[1]. This approach has been applied in plants under the global slow-fast leaf economic spectrum which describes investment and return of carbon and nutrients in leaves[1]. Whether this applies to other taxa, indicating general principles, remains untested. We advance generality in economic theories of life by showing that a slow-fast spectrum captures the resource economics of a globally dominant group of superorganisms, the ants. Like plants, ants acquire resources through modular units, the workers. Here, we collect traits from ant workers of 123 species across large-scale environmental gradients. Ants trade-off investment in biomass, chemical elements (nitrogen, phosphorus), energy (metabolic rate) and worker number, against assimilation rates (resource revenue) and lifespan. This superorganism economic spectrum does not vary across environmental gradients, rather, both slow and fast strategies persist amongst co-occurring species. High phylogenetic conservatism suggests early lineages of ants diverged in their economic strategies and subsequently diversified, locking in fundamental templates of investment and resource return. The remarkable similarities in economic strategies employed by ants and plants for resource acquisition and use suggest that there may be common principles underlying the rules of life.

Introduction

One of the basic principles common to all life is that organisms are sustained by the storage and turnover of energy (for fuelling metabolism) and chemical elements (for constructing biomass). Theory posits that organisms trade-off allocation of these resources to assimilation, growth and reproduction and that the pace of life follows a fast-slow continuum[2-4]. Resource assimilation is foundational to growth and reproduction[4] and can be framed using economic concepts of investment and return[5]. These ideas have been strongly developed in plants. In particular, the Leaf Economics Spectrum (LES) scheme[1] underpins current understanding of plant investment strategies: globally, plant species vary from having cheap but 'fast' leaves with high nutrient concentrations of nitrogen and phosphorus, high metabolic rates, rapid assimilation of resources, and short lifespans, to expensive but 'slow' leaves that are more robust with slow assimilation and metabolic rates and long lifespans. Here we ask, does this economic theory developed and tested in plants apply to other taxa?

We advance generality in economic theories of life by testing if the leaf economics spectrum applies to ecology's movers and shakers, the superorganisms[6]. Superorganisms, such as ants and other social insects (bees, wasps, termites), form colonies with distinct reproductive and non-reproductive members. Like plants, superorganisms are unique amongst the earth's biota because they assign resource acquisition to distinct modular units: in plants, to leaves and roots, and for superorganisms, their workers[7]. Superorganism workers gather and recycle the planet's resources at a vast scale, playing key roles in ecosystem processes, from seed dispersal to nutrient cycling and predation[6,8-10]. Such large-scale collective action requires balance between the construction and maintenance costs of workers and their resource income[7]. So, are superorganisms such as ants following the same economic rules as plants?

We tested for a worker economic spectrum in ants across seven subfamily clades including the five most globally diverse subfamily lineages[11]. We acquired trait data from individual workers from species sampled across extensive climatic and soil phosphorus gradients (Extended data Fig. 1, Table 1). Six of these traits directly parallel those used in the leaf economics spectrum[12]: body tissue N and P concentrations[13] and mass density (mass:volume ratio)[14], representing *investment costs*; mass-specific standard metabolic rate[15], representing *maintenance costs*; mass-specific assimilation

rate representing *potential revenue*; and worker lifespan[16] (*duration of the revenue stream*), which should be *optimised* to balance the lifetime net resource costs and benefits[17]. We also include worker body mass and worker number (colony size), two traits that can be altered to change overall colony mass thereby setting limits on the total colony budget[18]. Using these data, we then ask whether there are evolutionary and biogeographic signatures to the worker economic spectrum.

The superorganism economic spectrum

We quantified the relationships among the eight economic traits and decomposed the portion of trait correlation associated with phylogeny (conserved trait correlation[19]) and that independent of phylogeny (non-phylogenetic) using multi response phylogenetic mixed models (MR-PMM; model summary Table S1)[19,20]. Ant economic traits showed strong phylogenetic correlations (Fig. 1a, b, Extended Data Table 2) and generally strong phylogenetic signal (average posterior mean λ across traits: 0.62, range: 0.36 – 0.84; Extended Data Fig. 2, Extended Data Table 3). Lifespan (mean λ = 0.36) and nitrogen (mean λ = 0.41) showed less phylogenetic signal. As well, %P and mass-specific assimilation rate had weaker phylogenetic correlations compared to other traits (Fig. 1b, Extended Data Table 2). Trait correlations independent of phylogeny were much weaker overall (Extended Data Table 2, Extended Data Fig. 2, 3).

Our analyses revealed two distinct sets of phylogenetically conserved co-varying traits that represent a clear trade-off in investment and resource return, forming a spectrum of slow-fast economic strategy (Fig. 1a, b). Species that invest more biomass and nitrogen in workers have small colonies of larger, longer-lived workers with lower maintenance costs (mass-specific metabolic rate), low %P (hypothesised to represent growth rate[13]), and slow rate of resource return (mass-specific assimilation rate) - a slow economic strategy (Fig. 1a, b). Species that invest less biomass and nitrogen into their workers have higher metabolic costs which sets the rate of resource uptake, thereby offsetting these maintenance costs by facilitating quick rates of return on revenue invested[21]. These species with a fast economic strategy achieve larger colony sizes made up of smaller workers with short lives and fast worker turnover (Fig. 1a, b).

Selection has therefore favoured workers that gather resources at a rate that reflects their investment costs and the duration of their revenue stream. Similarly, under optimal lifespan theory[17], leaves

106 maximise average net resource carbon gain over the leaf life cycle[22]. Consequently, some trait
107 combinations will be rare or never observed[23]. For example, tough leaves, or robust ant workers with
108 short lifespans, will not have enough photosynthetic/foraging time to pay off high resource investment,
109 and hence these trait combinations are not favoured by natural selection.

110 **Biophysical laws constrain the economic spectrum**

111 The independent component of trait-trait relationships (not associated with phylogenetic history)
112 revealed three notable correlations that are likely to be driven by fundamental biophysical principles
113 dictating energy-mass balance [4,21]. Mass-specific metabolic and assimilation rates showed an
114 allometric negative relationship with body mass for both phylogenetic (Fig. 1a, b) and independent
115 trait correlations (Extended Data Table 2, Extended Data Fig. 3). From cells, to organisms, to
116 superorganisms[15], metabolic rate (*B*) scales allometrically with mass, according to a power function B
117 $= aM^{\beta}$ where, β is typically less than 1 (>-1 and <0 when mass-specific). Here, the mean slope of the
118 independent component of these relationships was -0.55 and -0.58 respectively indicating that smaller
119 workers have higher mass-specific metabolic and assimilation rates than larger workers (Extended
120 Data Table 2). Metabolic rate subsequently sets the rate of uptake of resources (assimilation rate)
121 from the environment[21] as demonstrated here with a positive phylogenetic (Fig. 1a, b) and
122 independent correlation (Extended Data Table 2, Extended Data Table Fig. 3) between these rates.

123 Several theories, with different underlying assumptions[24], have proposed that physio-chemical factors
124 place fundamental mass-based constraints on the metabolic and assimilation rates of organisms[24].
125 These constraints are hypothesised to relate to either nutrient supply networks (the basis of metabolic
126 theory of ecology[21]) or to surface-area scaling dynamics of energy reserve pools and volume of
127 structural biomass (dynamic energy budget theory[4]). The non-phylogenetic proportion of these
128 correlations is therefore likely due to these immutable design constraints independent of evolutionary
129 optimisation[24]. These constraints may limit the expansion of economic strategy space.

130 **Clades partition economic strategy space**

131 The superorganism economic spectrum occurs over two axes of variation. In multidimensional trait
132 space, the first axis represented the ant worker economic spectrum (AWES) explaining 61% of
133 variance. This axis was characterised by the correlation between biomass investment and lifespan
134 trading off against mass-specific metabolic rate, mass-specific assimilation rate, and colony size (Fig.

2). The second axis of variation represented a stoichiometry spectrum (SS), represented by the trade-off of N and P explaining 13% of variance. This shows a distinct departure from the leaf economics spectrum in which N and P in plant leaves are positively correlated, and co-vary with other LES traits over one axis of variation[1]. The N-P trade-off in ants aligns with ecological stoichiometry theory[25]. Nitrogen creates biological structure, while phosphorus is a critical component of the protein synthesis machinery (RNA-P) that fuels growth[25]. Nitrogen and phosphorus thereby act as opposing levers on growth rate for small metazoans[13].

The subfamilies of ants have evolved to occupy distinct regions of multidimensional economic strategy space (MANOVA – Axis 1: $F = 26.86$, $p < 0.0001$, Axis 2: $F = 16.02$, $p < 0.0001$, Fig. 2). For example, the three most globally diverse ant clades (Formicinae, Dolichoderinae, Myrmicinae) mostly occupy the fast end of the ant worker economic spectrum (Fig. 2). Within that, Myrmicinae are placed on the slower end of the stoichiometry spectrum (Fig. 2) with higher N content (indicative of thicker, more robust cuticles[14]) compared with Dolichoderinae, which in turn have shorter lifespans, and smaller body sizes than the Formicinae. Some genera we tested here include *Solenopsis* and *Pheidole*, that were on the fast end of the ant worker economic spectrum. These genera contain some of the world's worst invasive species[26]. Hence, there are clear prospects for applying the superorganism economic spectrum to global change research[27] as it provides a mechanistic basis to the impact of superorganisms (such as pest species) on our ecosystems and agriculture.

Full economic spectrum persists in all environments

We found no evidence that economic strategies are modulated by the environment: site-level climate and soil phosphorus were not significantly related to any of the response traits (MR-PMM trait:fixed effects, average p-value = 0.7, Table S1). Further, the two axes of variation in economic strategy (Fig. 2) were also not related to climate and soil phosphorus variables (Extended Data Table 4). In fact, the full suite of economic strategies was present in all environmental conditions tested (Extended Data Fig. 4). Similar global patterns are found in plants: although some leaf traits have strong relationships with climate (e.g., leaf mass per area with aridity[28]), trait coordination is largely independent of climate[1]. Therefore, for both ants and plants, much of the economic variation in trait relationships occurs amongst co-existing species.

Conclusion

We have described a phylogenetically conserved economic spectrum for a globally dominant group of superorganisms which is largely independent of climate and environmental effects. Our results suggest that early lineages of ants likely diverged in their economic strategies and subsequently diversified[11], thereby locking in these fundamental templates of investment and resource return. Although we quantified the economic spectrum using Australian species only, these species represent six globally widespread subfamilies. Given the strong role of evolutionary history compared to climate and environmental effects on the ant worker economic spectrum, we expect more globally extensive sampling would align with our key results. Some subfamilies, however, may shift in relative position along the spectrum due to behavioural differences when considering global data (Fig. 2). For example, Australian species of Dorylinae we tested here demonstrated a slow strategy as specialist predators with small stationary colonies (Fig. 2). In contrast, the nomadic army ants (Dorylinae) of South America and Africa have swarms of several hundred thousand workers that target generalised prey *en masse*[29], and may therefore hold a different strategy position along the economic spectrum.

Workers of social insect colonies gather resources across vast scales and have major impacts on habitats across our planet. Globally, ants can increase crop yields through their positive role on soil health[6], managed bee colonies pollinate one third of our crops[30] and termites decompose more than half of the deadwood in tropical forests[8]. Our economic framework has clear potential for modelling the resource economics of other social insects. It could be scaled up to address questions of invasive social insect dynamics and to predict the consequences of global change for the world's functionally vital superorganisms [31]. For researchers wishing to quantify the economic spectrum with a reduced number of traits, we suggest mass density (parallel to leaf mass per area) and %N would be a good starting point. These traits were central to the correlation network (Fig. 1b) and were relatively easy to collect at scale. A major goal of ecology is to identify broadly applicable principles that provide a mechanistic understanding of how living things behave. Our findings show that evolutionary optimisation and the biophysical laws of energy and mass balance have jointly shaped the economics of superorganisms and plants in similar ways indicating common solutions to resource allocation problems across the tree of life.

References

1 Wright, I. J. *et al.* The worldwide leaf economics spectrum. *Nature* **428**, 821-827 (2004).

2 Mathot, K. J. & Frankenhuis, W. E. Models of pace-of-life syndromes (POLS): a systematic review. *Behavioral Ecology and Sociobiology* **72**, 41 (2018). https://doi.org:10.1007/s00265-018-2459-9

3 Burger, J. R., Hou, C., Hall, C. A. & Brown, J. H. Universal rules of life: metabolic rates, biological times and the equal fitness paradigm. *Ecology Letters* **24**, 1262-1281 (2021). https://doi.org:https://doi.org/10.1111/ele.13715

4 Kooijman, S. A. L. M. *Dynamic energy budget theory for metabolic organisation*. (Cambridge university press, 2010).

5 Junker, R. R. *et al.* Towards an animal economics spectrum for ecosystem research. *Functional Ecology* **00**, 1-16 (2022).

6 Wu, D., Du, E., Eisenhauer, N., Mathieu, J. & Chu, C. Global engineering effects of soil invertebrates on ecosystem functions. *Nature* (2025). https://doi.org:10.1038/s41586-025-08594-y

7 Oster, G. & Wilson, E. *Caste and ecology in the social insects*. (Princteon University Press, 1979).

8 Griffiths, H. M., Ashton, L. A., Evans, T. A., Parr, C. L. & Eggleton, P. Termites can decompose more than half of deadwood in tropical rainforest. *Current Biology* **29**, 118-119 (2019).

9 Griffiths, H. M. *et al.* Ants are the major agents of resource removal from tropical rainforests. *Journal of Animal Ecology* **87**, 293-300 (2018). https://doi.org:https://doi.org/10.1111/1365-2656.12728

10 Klein, A.-M. *et al.* Importance of pollinators in changing landscapes for world crops. *Proceedings of the Royal Society B: Biological Sciences* **274**, 303-313 (2007). https://doi.org:doi:10.1098/rspb.2006.3721

11 Moreau, C. S., Bell, C. D., Vila, R., Archibald, S. B. & Pierce, N. E. Phylogeny of the Ants: Diversification in the Age of Angiosperms. *Science* **312**, 101-104 (2006). https://doi.org:doi:10.1126/science.1124891

12 Gibb, H. *et al.* Ecological strategies of (pl)ants: Towards a world-wide worker economic spectrum for ants. *Functional Ecology* **37**, 13-25 (2023). https://doi.org:https://doi.org/10.1111/1365-2435.14135

13 Elser, J. J. *et al.* Growth rate–stoichiometry couplings in diverse biota. *Ecology Letters* **6**, 936-943 (2003). https://doi.org:https://doi.org/10.1046/j.1461-0248.2003.00518.x

14 Peeters, C., Molet, M., Lin, C.-C. & Billen, J. Evolution of cheaper workers in ants: a comparative study of exoskeleton thickness. *Biological Journal of the Linnean Society* **121**, 556-563 (2017).

15 Shik, J. Z., Hou, C., Kay, A., Kaspari, M. & Gillooly, J. F. Towards a general life-history model of the superorganism: predicting the survival, growth and reproduction of ant societies. *Biology Letters* **8**, 1059-1062 (2012). https://doi.org:doi:10.1098/rsbl.2012.0463

16 Kramer, B. H., van Doorn, G. S., Arani, B. M. S. & Pen, I. D. Eusociality and the Evolution of Aging in Superorganisms. *American Naturalist* **200**, 63-80 (2022). https://doi.org:10.1086/719666

17 Kikuzawa, K. A cost-benefit analysis of leaf habit and leaf longevity of trees and their geographical pattern. *The American Naturalist* **138**, 1250-1263 (1991).

18 Kaspari, M. Global energy gradients and size in colonial organisms: worker mass and worker number in ant colonies. *Proceedings of the National Academy of Sciences* **102**, 5079-5083 (2005).

19 Westoby, M., Yates, L., Holland, B. & Halliwell, B. Phylogenetically conservative trait correlation: Quantification and interpretation. *Journal of Ecology* **111**, 2105-2117 (2023). https://doi.org:https://doi.org/10.1111/1365-2745.14150

20 Halliwell, B., Yates, L. A. & Holland, B. R. Multi-Response Phylogenetic Mixed Models: Concepts and Application. *Biological Reviews* (2022). https://doi.org:10.1101/2022.12.13.520338

21 Brown, J. H., Gillooly, J. F., Allen, A. P., Savage, V. M. & West, G. B. Toward a metabolic theory of ecology. *Ecology* **85**, 1771-1789 (2004).

22 Wang, H. *et al.* Leaf economics fundamentals explained by optimality principles. *Science Advances* **9**, eadd5667 (2023).

23 Castorena, M., Olson, M. E., Enquist, B. J. & Fajardo, A. Toward a general theory of plant carbon economics. *Trends in Ecology & Evolution* **37**, 829-837 (2022). https://doi.org:https://doi.org/10.1016/j.tree.2022.05.007

24 Maino, J. L., Kearney, M. R., Nisbet, R. M. & Kooijman, S. A. Reconciling theories for metabolic scaling. *Journal of Animal Ecology* **83**, 20-29 (2014).

25 Gillooly, J. F. *et al.* The metabolic basis of whole-organism RNA and phosphorus content. *Proceedings of the National Academy of Sciences* **102**, 11923-11927 (2005).

26 Cuthbert, R. N., Diagne, C., Haubrock, P. J., Turbelin, A. J. & Courchamp, F. Are the “100 of the world’s worst” invasive species also the costliest? *Biological Invasions* **24**, 1895-1904 (2022).

27 Bertelsmeier, C. *et al.* Different behavioural strategies among seven highly invasive ant species. *Biological invasions* **17**, 2491-2503 (2015).

28 Niinemets, Ü. Global-scale climatic controls of leaf dry mass per area, density, and thickness in trees and shrubs. *Ecology* **82**, 453-469 (2001).

29 Brady, S. G., Fisher, B. L., Schultz, T. R. & Ward, P. S. The rise of army ants and their relatives: diversification of specialized predatory doryline ants. *BMC Evolutionary Biology* **14**, 1-14 (2014).

30 FAOSTAT. ProdSTAT Database. **2022**, 09-28-22 (2022). <https://www.fao.org/faostat/en/#data/QCL>.

31 Elizalde, L. *et al.* The ecosystem services provided by social insects: traits, management tools and knowledge gaps. *Biological Reviews* **95**, 1418-1441 (2020). https://doi.org:https://doi.org/10.1111/brv.12616

261

262 **Figures**

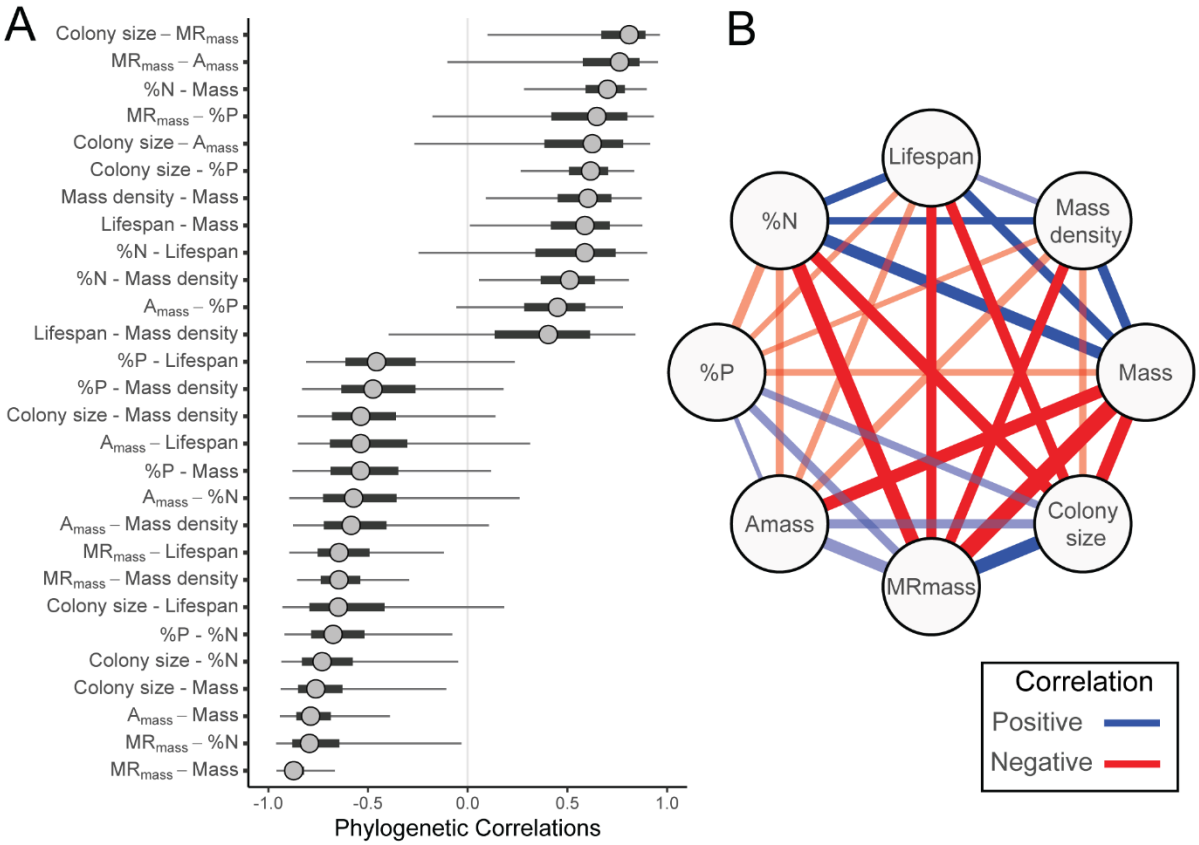

263

264 Figure 1: Two sets of correlated traits trade-off to create a slow-fast economic spectrum. (A) Posterior
265 summaries of phylogenetic correlation coefficients from MR-PMM analysis, showing the posterior
266 mean (point), 50% (heavy wick) and 95% (light wick) credible intervals. (B) Network diagram showing
267 phylogenetic trait correlations significant at 95% (bold) and 50-95% (faded) credible interval. Blue
268 lines = positive relationships, red lines = negative relationships. Line width indicates strength of
269 correlation. A_{mass} = mass-specific resource assimilation, MR_{mass} = mass-specific metabolic rate.

270

271

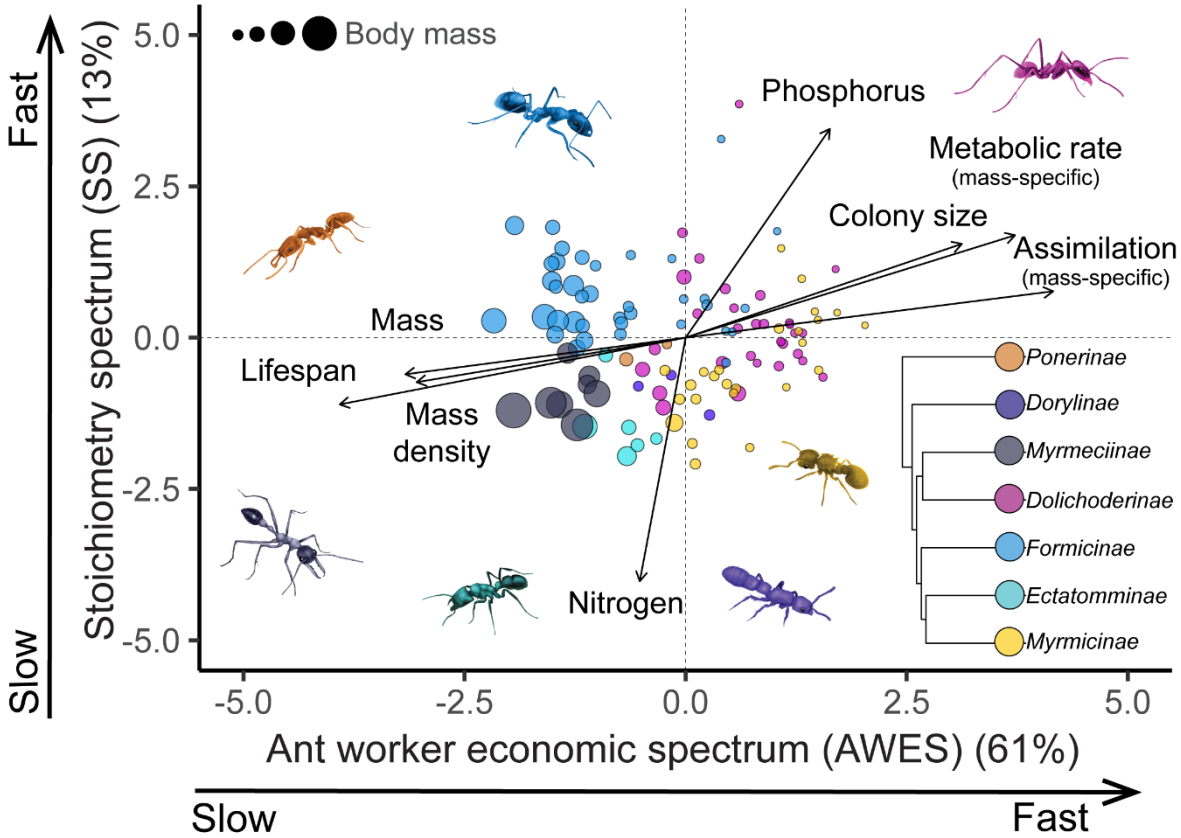

Figure 2: Mapping the superorganism economic spectrum onto multidimensional space. Showing varimax-rotated PCA from gap-filled species-averaged trait data from 305 colonies, with the 123 species as points and coloured as subfamily groups. Percentage variation explained in brackets for axis 1 (ant worker economic spectrum - AWES) and axis 2 (stoichiometry spectrum - SS). Size of points represents dry body mass scaled between 1-10. Ant icons are representative genera from each subfamily, anticlockwise from top left: Formicinae = *Camponotus*, Ponerinae = *Anochetus*, Myrmeciinae = *Myrmecia*, Ectatomminae = *Rhytidoponera*, Dorylinae = *Lioponera*, Myrmicinae = *Melanoplus*, Dolichoderinae = *Iridomyrmex*.

Extended data: The economic strategies of superorganisms

8 Figures/tables

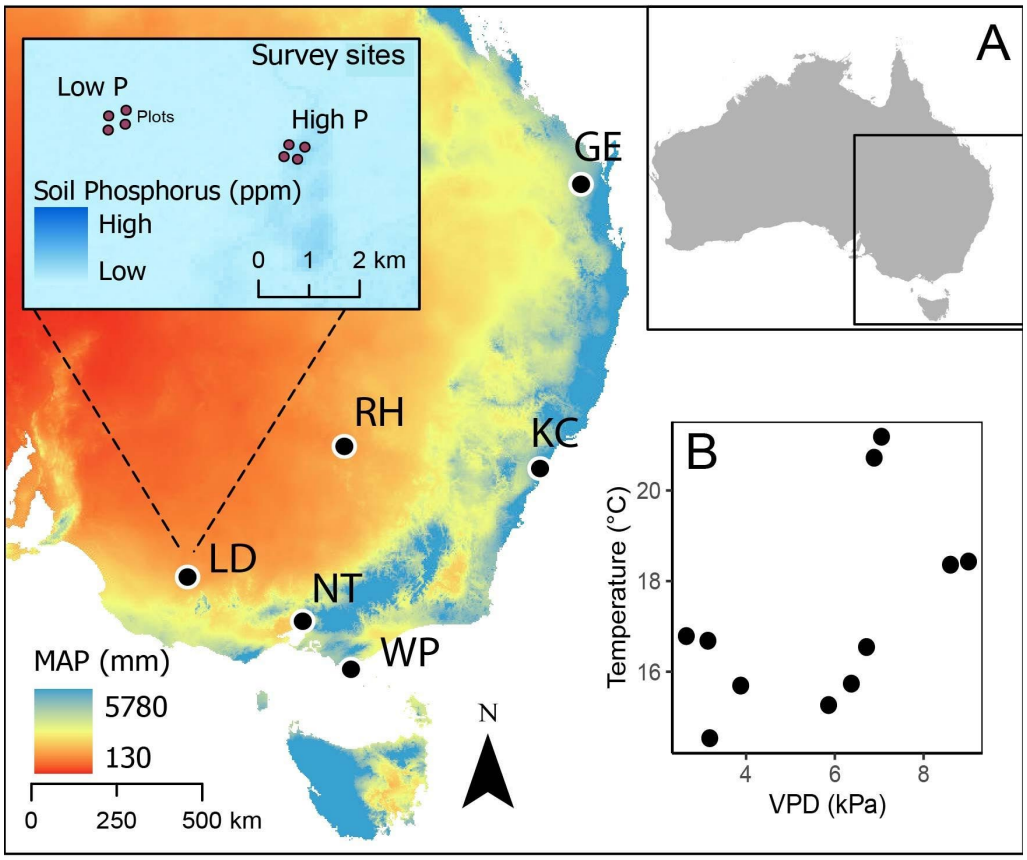

Extended data figure 1: A) Map of six locations representing low to high precipitation and temperature across the south-eastern region of Australia, inset indicates layout of sites (high phosphorus and low phosphorus) and plot survey design within each location, all locations were represented by two sites expect for NT represented by one high phosphorus site (total sites = 11), WP = Wilson's Promontory, KC = Ku-ring-gai Chase National Park, GE = Glen Echo, NT = Nangak Tamboree Wildlife Sanctuary, LD = Little Desert National Park, RH = Round Hill Nature Reserve, B) Mean annual microclimate temperature (T_m) and vapor pressure deficit (VPD_m) for eleven sites.

Extended data table 1: Economic traits of worker ants, abbreviations, units, % trait coverage across species sampled (n = 123), and equivalent trait in the Leaf Economics Spectrum (LES).

Trait	Term	Units	% coverage	Parallel to LES
Worker mass density	Mass density	mg/mm^3	94.31	Leaf mass per unit area
Mass-specific assimilation rate	A_{mass}	mg/day/mg	13.82	Photosynthetic capacity
Worker N concentration	N	%	92.68	Leaf N concentration
Worker P concentration	P	%	28.46	Leaf P concentration
Mass-specific metabolic rate	MR_{mass}	µW/hr/mg	91.06	Dark respiration
Lifespan	Lifespan	days	54.47	Lifespan
Colony size	Colony size	No. workers	13.82	NA
Body mass	Mass	mg	94.31	NA

Extended data table 2. Mean posterior correlation coefficients from multi-response phylogenetic mixed model (Table S2). Showing the phylogenetic correlation (upper triangular) and independent correlation (lower triangular) of each pairwise trait combination. Significance at 95% credible interval (CI) indicated by *****, correlations significant at 50-90% CI shown in bold.

	Mass	Mass density	Lifespan	% N	% P	A_{mass}	MR_{mass}	Colony size
Mass		**0.60***	**0.57***	**0.68***	**-0.46**	**-0.72***	**-0.86***	**-0.70***
Mass density	0.13		**0.42**	**0.49***	**-0.41**	**-0.54**	**-0.63***	**-0.49**
Lifespan	0.09	-0.09		**0.55***	**-0.43**	**-0.49**	**-0.61***	**-0.63***
% N	0.16	0.02	0.01		**-0.57**	**-0.51**	**-0.76***	**-0.67***
% P	-0.24	-0.15	-0.02	-0.07		**0.35**	**0.54**	**0.51**
A_{mass}	**-0.58**	-0.12	-0.009	-0.14	0.18		**0.67**	**0.57**
MR_{mass}	**-0.55***	-0.11	-0.04	-0.19	0.17	**0.46**		**0.74***
Colony size	0.18	0.08	-0.03	0.04	-0.07	-0.18		

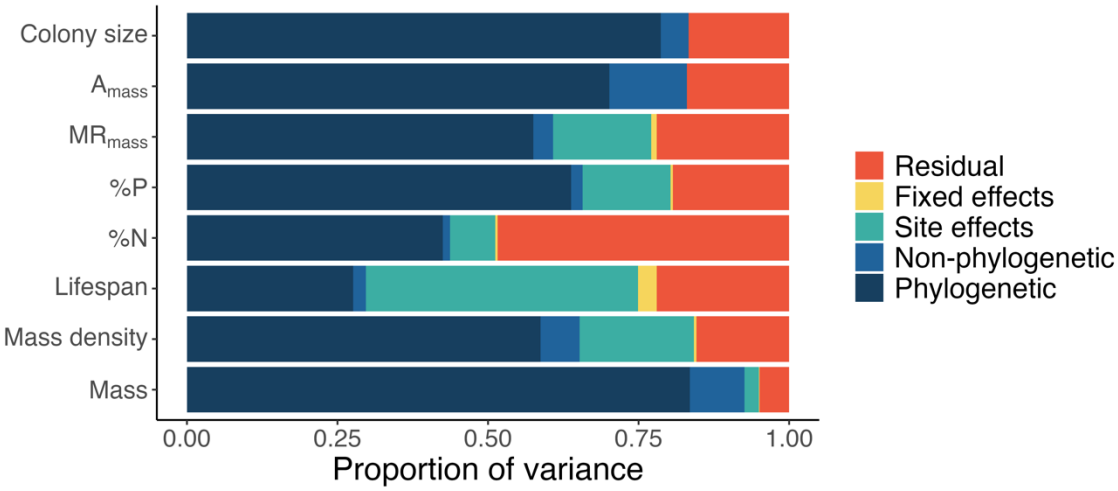

Extended data figure 2: Decomposition of trait variance (partial R^2) attributed to different levels in the model hierarchy. Phylogenetic = phylogenetically structured between-genus effects. Non-phylogenetic = non-phylogenetic (independent) between-species effects. Site effects = between survey locations. Fixed effects = variables of site-specific mean annual microclimate temperature, mean annual microclimate vapor pressure deficit (representing aridity), and soil phosphorus. Residual = residual variance unexplained by the model.

Extended data table 3: Posterior quantiles (0.5, 0.025, 0.975) of phylogenetic signal (λ) for each economic trait.

Trait	λ (±95% CI)
Mass	0.84 (0.69 – 0.91)
Mass density	0.63 (0.29 – 0.80)
Lifespan	0.36 (0.09 – 0.63)
Phosphorus	0.65 (0.23 – 0.89)
Nitrogen	0.41 (0.16 – 0.66)
A_{mass}	0.68 (0.30 – 0.89)
MR_{mass}	0.62 (0.28 – 0.78)
Colony size	0.77 (0.42 – 0.93)

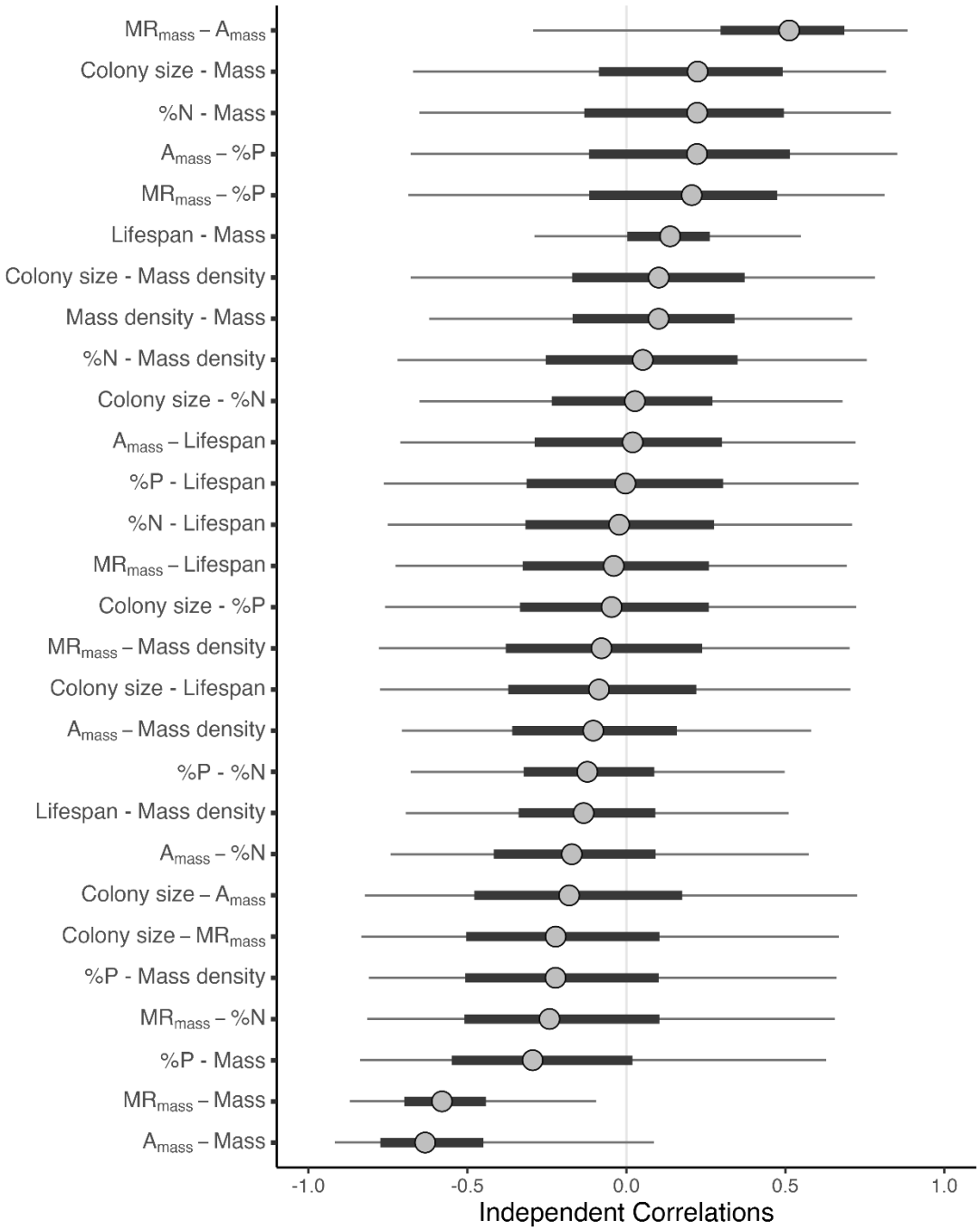

Extended data figure 3. Posterior summaries of independent (non-phylogenetic) correlation coefficients from multi-response phylogenetic mixed model showing the posterior mean (point), 50% (heavy wick) and 95% (light wick) credible intervals.

Extended data table 4: Linear OLS models of varimax-rotated PCA axes 1 and 2 representing two dimensions of the worker economic spectrum with climate and soil phosphorus as predictor variables.

Model	Adj. R^2	Coef. (± SE)	p-value
Axis 1 ~ $\log_{10}$ (Soil P)	0.01	-0.10 (0.07)	0.153
Axis 2 ~ $\log_{10}$ (Soil P)	0.01	0.09 (0.07)	0.192
Axis 1 ~ MAT_m	0.01	-1.05 (0.81)	0.199
Axis 2 ~ MAT_m	0.00	0.23 (0.82)	0.783
Axis 1 ~ VPD_m	0.00	-0.09 (0.24)	0.707
Axis 2 ~ VPD_m	0.00	0.12 (0.24)	0.611

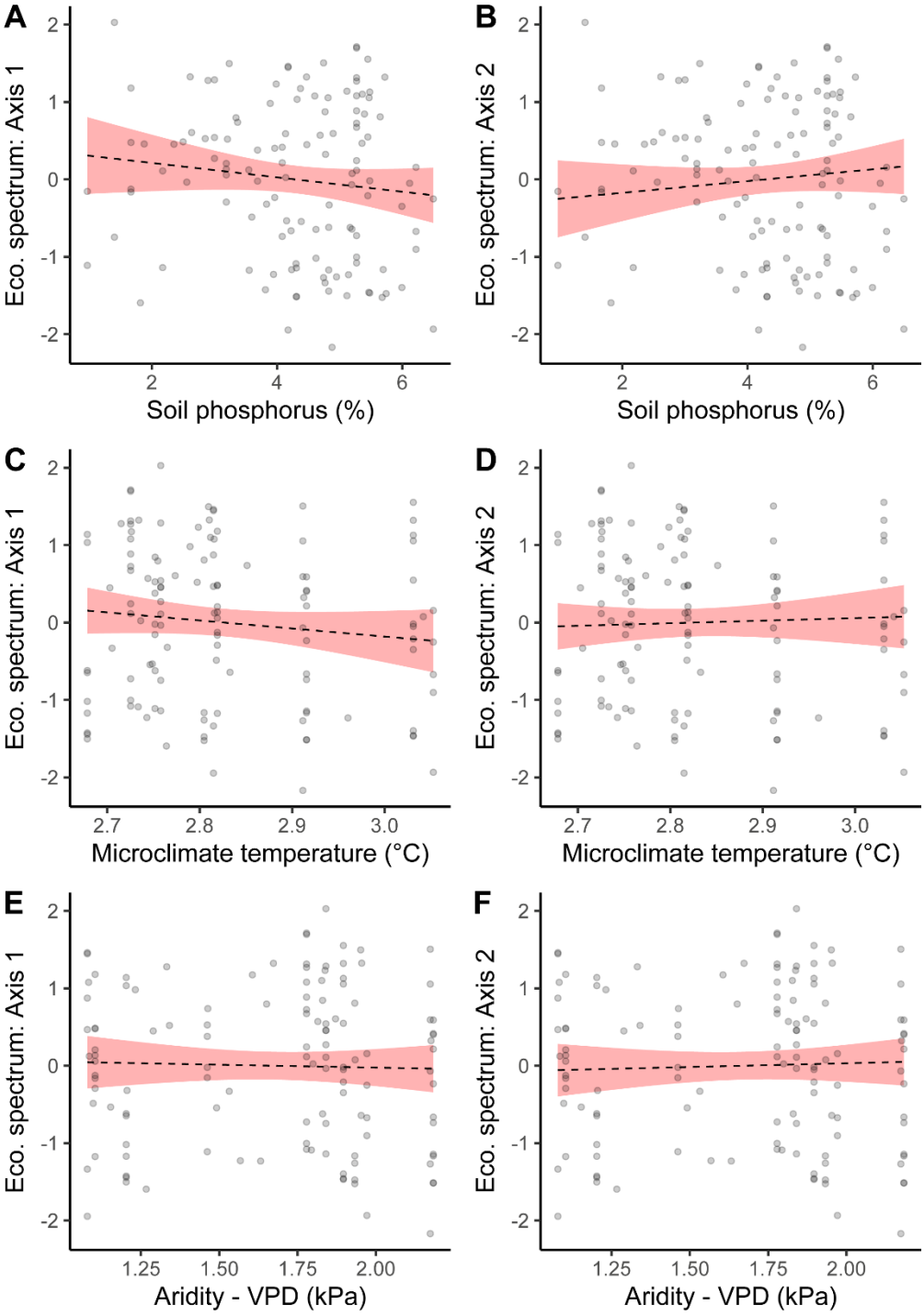

Extended data figure 4: The worker economic spectrum does not vary with climate and soil phosphorus. Showing varimax-rotated PCA axes 1 and 2 representing two dimensions of the worker economic spectrum with climate and soil phosphorus as predictor variables, points represent species, lines and 95% CI from model fits (Table S5). Microclimate temperature (MATm) is mean annual microclimate. Aridity gradient represented by microclimate vapor pressure deficit (VPDm).

Methods

Field locations

Ants were sampled from six locations along the east coast and inland of south-eastern Australia (Extended data Fig.1) representing a gradient of low to high aridity (421 – 1283 mm annual precipitation) and temperature (13 – 20 ˚C mean annual temperature). Locations were each sampled over a one-week period between June 2022 to April 2023. Within each location, two sites with contrasting soil phosphorus status were chosen using the CSIRO Soil and Landscape Grid National Soil Attribute Map – Total Phosphorus (3” resolution) release 1.V5 (Viscarra Rossel et al. 2014). Within each high P and low P site, four plots (10 x 10 m) separated by ~200 m, were established (total of eight plots per site). Soil phosphorus status of the plots was confirmed using soil chemical analysis. Nine soil cores (~5 cm diameter, 15 cm deep) were taken per plot, combined, and air-dried giving one soil sample per plot. Soil P was assessed through soil chemical analysis of Total P (17C1 Aqua regia block digestion; Rayment and Lyons (2011)) at Environmental Analysis Laboratory, Southern Cross University.

Ant field sampling

Each plot was comprehensively sampled for ants for two, one-hour blocks over two days such that each plot was surveyed in both the morning (~0900 – 1300 hrs) and afternoon (1300 – 1700 hrs). A final day of sampling was undertaken targeting specific plots to increase the number of species and colony replicates. Ten baits in 5 ml plastic vials, five with tuna, five with honey, were placed on the ground along a 50 m transect at the beginning of the search to attract foraging ants. Ants were collected from baits if they had formed a clear foraging trail which indicated the individuals were from the same colony. Hand searches involved locating nests by checking under rocks, logs, tussocks, coarse woody debris, and vegetation and looking for ant foraging trails. Ants foraging arboreally in columns were assumed to be from the same colony and were sampled using aspirators or brushing ants into a container with a paint brush. To lure ants from nests that were difficult to access, another five to ten traps of each bait type were placed at nest entrances.

Climate data

We modelled microclimate for the sites using the *micro_ncep* function in package NicheMap R for the years 2009-2023[1]. This function uses the *microclima* package[2] as well as the RNCEP [3] and elevatr[4] packages to connect to the 6-hourly 2.5 x 2.5-degree gridded historical NCEP data (global scope). It then downscales climate to hourly estimates accounting for local terrain effects (~30 x 30 m) including elevation-induced lapse rates, coastal influences and cold-air drainage[1]. We parametrised the model for each site using shade values which were obtained from field vegetation surveys. For each plot, nine 50 cm^2 quadrats were placed at random and % cover of canopy, understorey, and shrub layer (where present) was recorded. The values were summed with the maximum value set at 100% cover. The values were then averaged per plot and then per site to provide a shade value. We used a single shade value per site-model. Default values were used for other parameters in the model. We extracted temperature (T) and relative humidity (RH) at 1.2 m standard height above the ground and averaged these values to get daily averages and the annual average across all 15 years. We calculated VPD as SVP(1-(RH/100)), where SVP was calculated as $610.78 \times e^{(T / (T + 237.3) \times 17.2694)}$[5].

Ant sampling

We aimed to collect as many ant species as possible from each site over three days of sampling. During sampling, live worker ants were collected either from foraging trails or nests using hand searches and baiting. We aimed to collect a minimum of 30 workers (and up to ~200 individuals) per colony, taken from 1-5 colony replicates per species per site. In the field, ants were allocated to morphospecies within genera or species complexes based on morphological observations using a microscope. Following field collection, 3-5 individuals from each colony were pinned and assigned a species or a species complex. Voucher specimens were deposited in the CSIRO TERC collection in Darwin, Australia, and the Gibb Lab collection at La Trobe University, Australia. Live field collected colonies were placed into plastic containers with the top 10 cm of the inner rim lined with fluon, given a honey-water mix (50:50) and hydration via a saturated cotton ball every two days and housed at 20˚C. Ants were transported back to the lab for trait measurements within 1-4 days from collection. Brood, alates, and major workers were collected but were not used for any trait analyses reported here. For polymorphic species (e.g. *Camponotus* or *Pheidole* species), we exclusively measured traits for minor workers.

Economic traits

Metabolic rate

Ants were housed as above while waiting to be trialled. Time between field collection and metabolic trials across sites ranged between 3-14 days. As digestion can influence metabolic rate, ants were starved but provided with water for 48 hours prior to trials. Carbon dioxide production (VCO_2) was used as a proxy for metabolic rate and was measured at a consistent temperature of 22˚C of using 8 Sable Systems International (SSI) multiple animal versatile energetics (MAVEn (SSI, Las Vegas, Nevada, USA)) systems, each attached to a Li-Cor 7000 CO_2/H_2O infrared gas analyser (Li-Cor, Lincoln, Nebraska, USA), housed in a Panasonic MIR 352H-PE climate control cabinet (Panasonic Healthcare, Sakata, Japan). Ants were placed in sets of 10 individual 2 ml or 3 ml curettes (depending on the size of the individual) with airstream humidity maintained at 90.34 ± 0.6% RH to avoid desiccation. Each ant was measured twice for a period of 10 minutes each time with a 5-minute baseline in between individuals to account for drift in the Li-Cor 7000 measurements. An additional 20 minutes was added at the beginning (for settling) and the end (as contingency). The activity of each ant was measured simultaneously as a unitless measurement using infrared light detectors in the MAVEn activity board.

Data treatment and extraction were conducted with the software Expedata (SSI). First VCO_2 data was corrected to standard temperature and pressure for a push system according to the equations of [6] and then baseline corrected using the Catmull-Rom spline method. To obtain standard metabolic rate (SMR) we then took the average of the lowest one minute of VCO_2 for each ant. VCO_2 was then inspected for outliers. Individuals with very high activity in the context of their respective colonies and species were removed (seven individuals). Individuals with erroneous values due to technical errors (e.g., temporary issues with flow rate) were removed (n = 103 individuals). We then systematically removed outliers that were 1.5 times the IQR of the data for each colony respectively (n = 184 individuals) as these could represent stressed or dying individuals. Finally, colonies with < 3 individuals remaining after these steps were removed from the dataset (n = 15 individuals). Together the outliers represented 9.56% of the original data resulting in a final dataset of 2805 individuals of 214 colonies of 114 species.

514 To explore whether activity during assays affected metabolic rate, we modelled VCO_2 as a function of
515 the activity variables in a linear mixed effects models with species, colony ID, and survey location as
516 random effects using the *lmer* function[7]. There was no significant relationship between total activity
517 over the assay and VCO_2, with random effects explaining all the variation in the model ($F = 0.11$, $p =$
518 0.740, $R_m^2 = 0.0002$, $R_c^2 = 0.72$). There was a significant relationship between activity at time of VCO_2
519 trace (slope of the absolute difference sum transformed activity (Slope ADS) and VCO_2 (slope ± 95%
520 CI: 0.54 (0.13 – 0.95), $p = 0.01$), but the fixed effect (Slope ADS) explained a very small amount of
521 variance in the model ($R_m^2 = 0.0014$, $R_c^2 = 0.72$). Therefore, we did not include individual activity
522 during assays as a covariate in downstream analyses. Minimum VCO_2/hr was then averaged per
523 colony and converted to microWatts/hr.

524 *Lifespan*

525 Lifespan was measured in the lab using a subset of species collected from each of the six field
526 locations. Following transport from the field to the lab, thirty workers per colony were transferred to
527 new plastic containers as a colony fragment and housed in a controlled temperature room at 25˚C
528 with humidity set to room ambient conditions. To simulate nest conditions and reduce stress, no light
529 was provided except during feeding and hydration periods. Colony fragments were placed in a
530 randomized position on the shelves to remove any location-specific effects of the controlled
531 temperature room environment. They were provided with a diet of honey-water mix (50:50) and dried
532 insects fed *ad libitum*, with hydration provided via a saturated cotton ball every two days. We
533 monitored colony fragments daily to record and remove deceased ants which were placed in 5 ml
534 tubes and instantly frozen at -20 °C. We ignored initial loss due to stress and began death counts 2
535 days after transfer to the controlled temperature room. Median survival time (in days) per colony was
536 calculated using survival curves fitted with the Kaplan-Meier estimate using the function *survfit* in
537 package "survival" (version 3.5-5) [8].

538 *Body mass*

539 Field collected colonies which were not allocated to either metabolic rate assays or lifespan assays
540 were immediately frozen at -20 °C upon collection from the field. All frozen ants (from metabolic
541 assays, lifespan assays, and directly from the field) were dried at 50 °C for 48 hours. We then
542 measured dry mass using a 0.001 mg precision XS3DU microbalance (Mettler Toledo). For ants from

metabolic and lifespan assays, dry mass was measured for each individual and the average per colony calculated, for the remaining colonies, dry mass was measured for 10 ants per colony and their average mass calculated.

Mass density

We calculated mass density of worker ants as density = mass/volume. Head volume was used as a proxy for body volume. Head volume was calculated using the formula for the volume of an ellipsoid as $V = 4/3\pi abc$, where a = head width (HW), b = head length (HL), and c = head height (HH). The heads of dried ants were removed and placed under a microscope to measure HW and HL of five to ten individuals per colony. Measurements were taken in mm using a Leica microscope camera and Leica Application Suite (LAS version 1.4). We note that ant heads are unlikely to shrink in volume with drying due to their thick cuticles (i.e. in comparison to softer bodied insects). Head height was difficult to measure at scale using this technique. We predicted that HH would be a proportion of HW, but this proportion would vary by genus due to different morphology (note head shape is likely to be constrained at genus level and is therefore unlikely to show much variation amongst species within a genus [9]). We used front and side profile photos of pinned ants obtained from AntWeb (California Academy of Science 2024) to calculate HH:HW as a proportion for each genus (n = 34) in the study. Using pinned AntWeb photos and imaging software Image J FIJI ver.1.54f [10] we measured HH and HW of 1-3 pinned individuals of three representative species (species were matched to the species in our dataset where possible) except for *Anochetus*, *Mesoponera*, and *Froggattella* which were represented by two species and *Paraparatrechina* which was represented by one species. We then calculated average HH:HW for each genus as a proportion between 0-1. HH:HW averaged 0.68 (± 0.08 SD) and ranged from 0.49 – 0.90. We then used the HH:HW proportion value per genus and the HW measurements from our dataset to estimate HH. Mass density of workers was then calculated as an average value per colony with units as mg/mm^3.

Nitrogen and phosphorus body concentrations

Dried ants (including removed heads) were combined per colony to undergo chemical analyses of nitrogen (%N) and phosphorus (%P). Gasters were removed prior to %N analysis as samples were simultaneously analysed for $\delta^{15}N$ which requires removal of recently consumed food located in the gaster[11] ($\delta^{15}N$ data not included in this study). Ant samples were analysed for nitrogen content (%N)

using the EA (Dumas) method performed using an Isoprime (Micromass, Wythenshawe, Manchester, U.K.) with a Carlo Erba CE1100 elemental analyser (Fisons, Milan, Italy) at the Isotope Facility of the Farquhar Laboratory of the Research School of Biology, Australian National University, ACT, Australia. Approximately 1 to 2 mg (to 3 µg precision) of each dried sample was weighed into a tin capsule. The Isoprime corrects for drift and time variable source effects using CO_2 and N_2 reference pulses. Post processing corrections were made using laboratory standard materials (cane sugar, beet sugar, cysteine and glycine). Inhouse software (SecondRat) was used to assess the results and correct to the standards. Ant samples were analysed for phosphorus content (%P) using 17C1 Aqua regia block digestion [12] conducted at the Environmental Analysis Laboratory, Southern Cross University. Dried ants were ground and ~100.0 mg of each sample was weighed and analysed. Test and reference samples were used to correct for any drift or carry-over in the instrument. The references were calibrated for total %P.

Colony size

At one field location (Nangak Tamboree Wildlife Sanctuary, Victoria), we undertook a mark-recapture study on ant colonies in the field to estimate colony size. To achieve phylogenetic representation, we sampled 17 species from 5 subfamilies and 10 genera, encompassing 34 colonies (2 colony replicates per species). We selected cohorts of 30 to 100 worker ants per colony, prioritizing similarity in worker size to minimise the impact of polymorphic body sizes. We marked workers on their gasters using coloured paint marker pens. Every three months we marked a new cohort for each colony with a new colour. Within a cohort, individual ants were indistinguishable by their markings. We conducted biweekly hour-long observations, pausing only during heavy rain, until a month passed without sighting any marked workers. In each session, we documented two primary variables: the total number of foraging ants and the count of marked workers. Observations were made between 8:00 to 19:00 depending on when each colony was active. Activity times of the ants were based on previous field observations at this location[13].

To estimate colony size for each species, we employed Chapman's estimator[14], a refinement of the Lincoln-Petersen estimator, using mark-recapture data. We excluded only the days where no ants were observed. Chapman's estimator was calculated for each coloured cohort per colony and for each observation day using the formula:

601 *Chapman= (M + 1)(C + 1)/ (R + 1) - 1*

602 where M is the total number of initially marked ants, C is the total number of ants observed on a
603 recapture day, and R is the number of marked ants recaptured on a recapture day. We averaged
604 these estimates of cohort size to derive a single colony size estimate.

605 *Assimilation rate*

606 We calculated assimilation rate for ant species from one field location (Nangak Tamboree Wildlife
607 Sanctuary). This was measured in the lab as part of a larger nutritional geometry study on the trophic
608 position of ants. We collected 30 individual workers from the same field colonies for which colony size
609 was estimated above (n = 17 species, 34 colonies). We transferred ants to plastic containers as a
610 colony fragment and housed them in a controlled temperature room at 25 ˚C with humidity set to room
611 ambient conditions. To simulate nest conditions and reduce stress no light was provided except during
612 feeding and hydration periods. We formulated three dietary options, each moulded into a cube, giving
613 different protein-to-carbohydrate (P:C) ratios: 1:3, 1:1, and 3:1. The diet cubes were prepared using a
614 standardized protocol to ensure consistency[15]. The experiment was conducted over six consecutive
615 days, with each 24-hour interval marking a measurement cycle. At the end of each period, the diet
616 cubes were weighed in their wet state, then dried for 48 hours at 60 ˚C and re-weighed to obtain a dry
617 weight. We calculated the total intake values combining carbohydrate and protein intake over a six-
618 day period. This rate was then divided by the number of workers in the colony fragment to give an
619 assimilation rate as mg food consumed per worker per day.

620 *Trait data coverage and treatment*

621 Trait coverage was uneven across species (n = 123), genera (n = 34), and subfamilies (n = 7)
622 (Extended data table 1). All traits were logged and scaled prior to analysis. Metabolic rate and
623 assimilation rate were divided by body mass to give mass-specific rates of μWatts/hr/mg worker and
624 mg food/day/mg worker respectively.

625 Statistical Analysis

626 *Multi-response phylogenetic mixed models*

627 We used Bayesian multi-response phylogenetic mixed models (MR-PMM) to decompose correlations
628 between species economic traits into phylogenetic and non-phylogenetic components[16]. Components

associated with phylogeny can be thought of as conservative trait correlation (CTC), where-as non-phylogenetic components can be thought of as trait correlations independent of phylogeny *sensu* Westoby et al.[17]. Multi-response models provide a more biologically appropriate model structure than traditional methods (i.e. PGLS, PICs) given that evolutionary selection on traits is often reciprocal rather than unidirectional, and adaptation often proceeds by phylogenetic niche conservatism[17]. We used trait data collected above from 305 colonies of 123 species from 11 environmental sites. Specifically, we fitted all economic traits jointly as response variables, removing the global intercept to estimate separate intercepts for each response, and using correlated random effects to specify phylogenetic and non-phylogenetic covariance matrices. We modelled multi-level structure in the data by fitting random intercepts across species (accounting for within-species replication), and sites (accounting for the sampling hierarchy). Parameter estimates from models are reported as posterior means with 50% and 95% credible intervals in Fig. 1a and Extended data Fig. 3 and with 50-95% credible interval (faded) and 95% credible intervals (bold) for Fig. 1b and indicated in Extended data Table 3.

In addition to estimating and decomposing correlations between response variables, we included site-level climate and soil P variables as fixed effect predictors of all response variables except A_{mass} and colony size (derived from collections at a single site and therefore invariant with respect to fixed effect predictors). These were downscaled microclimate mean annual temperature (MAT_m) and microclimate mean annual VPD (VPD_m) which were interpolated at the site level (11 sites across six locations – see above “Climate data”) and soil phosphorus (soil phosphorus) which was measured at the plot level (n = 38 plots, note 3 plots did not have sufficient ants collected for trait measurements). Climate and soil P variables were not significantly correlated (pairwise correlations all $p > 0.05$) and therefore did not pose issues of multicollinearity. All MR-PMM were fit using the MCMCglmm R package (Hadfield 2010).

A genus-level phylogenetic tree was used to derive the phylogenetic correlation matrix for all analyses. This approach treats species as replicates of a genus when estimating phylogenetic random effects and therefore ignores any phylogenetic structure between species within ant genera. We chose this approach because species level phylogenetic relationships are not well resolved for most Australasian ant taxa. We constructed a genus-level phylogenetic tree using a time-calibrated

659 phylogeny, which includes several representative species of each genus worldwide[18]. We pruned the
660 tree to the 34 genera included in our study using 'drop.tip' from *ape* ver 5.3 [19], and inserted three
661 additional genera using 'bind.tip' from *phytools* [20]. Genera *Lioponera* and *Zasphinctus* (the only
662 representative genera of Dorylinae included in the study) were placed as sister genera to *Cerapachys*
663 [21] (*Cerapachys* was then dropped from the tree). Genus *Chelaner* was placed as sister to
664 *Monomorium* [22].

665 *Model Fitting*

666 We used parameter expanded priors with (variance) $V = I_k$ (an identity matrix of dimension equal to
667 the number of response traits, k), and (degree of belief) v = k+1 for random effects[23], and default
668 independent normal priors with (mean) = 0 and $V = 10^{10}$ for fixed effects. Estimates for all parameters
669 converged successfully with nitts = 110000, burn-in = 10000, and thin = 100. We assessed model
670 convergence from 4 separate MCMC chains by 1) visually inspecting traces of the MCMC posterior
671 estimates; and 2) confirming potential scale reduction factors ($\hat{r}$), a convergence diagnostic test that
672 compares within- and between-chain variance [24], were <1.01 for all parameter estimates (Fig. S1).
673

674 *Model Validation*

675 We performed model validation using posterior predictive checks and a leave-one-out (LOO) cross-
676 validation (CV) procedure. Specifically, we performed LOO-CV at the species level, by leaving one
677 species out per model fit when calculating the log predictive density. Posterior predictive checks
678 confirm that the fitted model generates plausible data for all response variables (Fig. S2). Predictions
679 from LOO-CV show that observed data for left-out species have good coverage at the 95% credible
680 interval and effectively estimate the rank order of species mean phenotypic values (Fig. S3). Further,
681 estimates of phylogenetic correlations derived from combining posterior samples across LOO-CV fits
682 had almost identical means and CIs (Fig. S4) to those fit to the full dataset (Fig.1a), indicating that
683 parameter estimates are robust to cross validation. Finally, we explored fitting the model with and
684 without phylogenetic components of trait (co)variance to assess the importance of phylogenetic
685 effects on model predictive performance. A model including phylogenetic (co)variances substantially
686 outperformed a model with no phylogenetic component based on leave one out cross-validation (Fig.
687 S5). Furthermore, LOO-CV predictions from this reduced model showed wide CIs and were unable to
688 capture the rank order of species phenotypic values (Fig. S3).

Phylogenetic signal

We calculated phylogenetic signal in each economic trait from the fitted MR-PMM as λ,

$$\lambda_i = \frac{\sigma_{ii}^{phy}}{\sigma_{ii}^{phy} + \sigma_{ii}^{ind} + \sigma_{ii}^{site} + \sigma_{ii}^{res}}$$

where $\sigma_{ii}^{phy}, \sigma_{ii}^{ind}, \sigma_{ii}^{site}, \sigma_{ii}^{res}$ and σ_{ii}^{res} are the estimated phylogenetic, non-phylogenetic, site, and residual variances for trait *i*, respectively.

Phylogenetic imputation

Traits varied in the extent of missing data (Extended data Table 2). Missing response values are permitted in MCMCglmm, with missing values imputed conditional on the full covariance structure of the model. In our case, this means that both phylogenetic and non-phylogenetic trait correlations inform the imputation of missing values[16,25]. One benefit of this approach over multiple imputation procedures is that imputation uncertainty is naturally propagated through to the posterior distribution of parameter estimates from the fitted model. We used the gap-filled dataset predicted from the MR-PMM fit to conduct a PCA (see section below and Fig. 2).

Principle components analysis

To examine how the economic traits map onto reduced dimensional space, and the spread of major subfamily clades across these dimensions, we used the gap-filled dataset to calculate species-means for each trait. Using these species trait averages we constructed a principle components analysis (PCA) with varimax rotated axes (to aid interpretation) using the function *principle* in the package 'psych' [26]. We coloured species points by subfamily mapped onto the first two PC axes to observe where the seven major subfamily clades were positioned within multi-trait space. We then tested whether variation along these axes of economic strategy was associated with climate and soil P, using linear regressions between PC components and each climate (T_m and VPD_m) and soil P variable (Extended data Table 4).

Data availability: Code sufficient to replicate all analyses and original data will be available at Figshare upon publication.

References

1 Kearney, M. R., Gillingham, P. K., Bramer, I., Duffy, J. P. & Maclean, I. M. D. A method for computing hourly, historical, terrain-corrected microclimate anywhere on earth. *Methods in Ecology and Evolution* **11**, 38-43 (2020). https://doi.org:https://doi.org/10.1111/2041-210X.13330

2 Maclean, I. M. D., Mosedale, J. R. & Bennie, J. J. Microclima: An r package for modelling meso- and microclimate. *Methods in Ecology and Evolution* **10**, 280-290 (2019). https://doi.org:https://doi.org/10.1111/2041-210X.13093

3 Kemp, M. U., Emiel van Loon, E., Shamoun-Baranes, J. & Bouten, W. RNCEP: global weather and climate data at your fingertips. *Methods in Ecology and Evolution* **3**, 65-70 (2012). https://doi.org:https://doi.org/10.1111/j.2041-210X.2011.00138.x

4 Hollister, J., Shah, T. & Beck, M. *jhollist/elevatr: Latest CRAN release (v0.1.3).* 2017).

5 Monteith, J. & Unsworth, M. *Principles of environmental physics: plants, animals, and the atmosphere*. (Academic press, 2013).

6 Lighton, J. R. *Measuring metabolic rates: a manual for scientists.* (Oxford University Press, 2018).

7 Bates, D., Maechler, M., Bolker, B. M. & Walker, S. Fitting Linear Mixed-Effects Models Using lme4. *Journal of Statistical Software* **67**, 1-48 (2015). https://doi.org:doi:10.18637/jss.v067.i01.

8 Therneau, T. A Package for Survival Analysis in R. **R package version 3.5-5** (2023). https://doi.org:https://CRAN.R-project.org/package=survival

9 Parr, C. L. *et al.* GlobalAnts: a new database on the geography of ant traits (Hymenoptera: Formicidae). *Insect Conservation and Diversity* **10**, 5-20 (2017). https://doi.org:https://doi.org/10.1111/icad.12211

10 Schindelin, J. *et al.* Fiji: an open-source platform for biological-image analysis. *Nature Methods* **9**, 676-682 (2012). https://doi.org:10.1038/nmeth.2019

11 Blüthgen, N., Gebauer, G. & Fiedler, K. Disentangling a rainforest food web using stable isotopes: dietary diversity in a species-rich ant community. *Oecologia* **137**, 426-435 (2003). https://doi.org:10.1007/s00442-003-1347-8

12 Rayment, G. E. & Lyons, D. J. *Soil chemical methods: Australasia*. Vol. 3 (CSIRO publishing, 2011).

13 Buxton, J. T., Robert, K. A., Marshall, A. T., Dutka, T. L. & Gibb, H. A cross-species test of the function of cuticular traits in ants (Hymenoptera: Formicidae). *Myrmecological News* **31** (2021).

14 Chapman, D. G. Some properties of the hypergeometric distribution with applications to zoological censuses. *Univ. Calif. Stat.* **1**, 60-131 (1951).

15 Krabbe, B. A. *et al.* Using nutritional geometry to define the fundamental macronutrient niche of the widespread invasive ant Monomorium pharaonis. *PLoS One* **14**, e0218764 (2019).

16 Halliwell, B., Yates, L. A. & Holland, B. R. Multi-Response Phylogenetic Mixed Models: Concepts and Application. *Biological Reviews* (2022). https://doi.org:10.1101/2022.12.13.520338

17 Westoby, M., Yates, L., Holland, B. & Halliwell, B. Phylogenetically conservative trait correlation: Quantification and interpretation. *Journal of Ecology* **111**, 2105-2117 (2023). https://doi.org:https://doi.org/10.1111/1365-2745.14150

18 Economo, E. P., Narula, N., Friedman, N. R., Weiser, M. D. & Guénard, B. Macroecology and macroevolution of the latitudinal diversity gradient in ants. *Nature Communications* **9**, 1778 (2018). https://doi.org:10.1038/s41467-018-04218-4

19 Paradis, E. & Schliep, K. ape 5.0: an environment for modern phylogenetics and evolutionary analyses in R. *Bioinformatics* **35**, 526-528 (2019).

20 Revell, L. J. phytools: an R package for phylogenetic comparative biology (and other things). *Methods in ecology and evolution* **3**, 217-223 (2012).

21 Borowiec, M. L. Generic revision of the ant subfamily Dorylinae (Hymenoptera, Formicidae). *ZooKeys*, 1 (2016).

22 Sparks, K. S., Andersen, A. N. & Austin, A. D. A multi-gene phylogeny of Australian *Monomorium* Mayr (Hymenoptera : Formicidae) results in reinterpretation of the genus and resurrection of *Chelaner* Emery. *Invertebrate Systematics* **33**, 225-236 (2019). https://doi.org:https://doi.org/10.1071/IS16080

23 de Villemereuil, P. Quantitative genetic methods depending on the nature of the phenotypic trait. *Annals of the New York Academy of Sciences* **1422**, 29-47 (2018).

24 Vehtari, A., Gelman, A., Simpson, D., Carpenter, B. & Bürkner, P.-C. Rank-normalization, folding, and localization: An improved R^for assessing convergence of MCMC (with discussion). *Bayesian analysis* **16**, 667-718 (2021).

25 Sanchez-Martinez, P. *et al.* A framework to study and predict functional trait syndromes using phylogenetic and environmental data. *Methods in Ecology and Evolution* **15**, 666-681 (2024). https://doi.org:https://doi.org/10.1111/2041-210X.14304

26 Revelle, W. *psych: Procedures for Psychological, Psychometric, and Personality Research*, <https://CRAN.R-project.org/package=psych> (2024).

Acknowledgements: We thank and acknowledge the Wurundjeri people of the Kulin Nation, the Wotjobaluk, the Ngiyampaa, the Durramurragal, the Gubbi Gubbi, the Boonwurung, Bunurong, and Gunaikurnai people on whose lands this field work was conducted. We thank Emily House for access to Glen Echo. Field work was carried out under Permit SL102675 NSW Department of Planning, Industry and Environment, Permit AA-0000328 Parks Victoria, and under animal ethics committee permit AEC22001.

Author Contributions: LL, HG, IJW conceptualized and designed the study with input from NJS, TRB, and CLP. LL, HLR, and AGC collected all trait data. BH analysed the data for the primary analysis and LL performed secondary analyses. LL wrote the manuscript with contributions from BH, HG, IJW, NJS, TRB, CLP, SLC, ANA. SLC provided equipment and technical support for metabolic assays. ANA provided taxonomic identification. Funding was acquired by HG and IJW.

Competing Interest Statement: There are no conflicts of interest.